Source Model of the Co- and Post-Seismic Deformation Associated with the 1994 far off Sanriku Earthquake (M7.5) Inferred from Strain and GPS Measurements

Tôhoku Geophys. Journ. (Sci. Rep. Tôhoku Univ., Ser. 5), Vol. 35, No. 1, pp. 15-32, 1998

Source Model of the Co- and Post-Seismic Deformation Associated with the 1994 far off Sanriku Earthquake (M7.5) Inferred from Strain and GPS Measurements

TAKUYA NISHIMURA[1]*, SATOSHI MIURA[1], KENJI TACHIBANA[1], KEIICHI HASHIMOTO[1], TOSHIYA SATO[1], SYUICHIRO HORI[1], EIJU MURAKAMI[1], TOSHIO KONO[1], KOICHI NIDA[1], MASAAKI MISHINA[1], TOMOWO HIRASAWA[1] and SHIN'ICHI MIYAZAKI[2]

(Received January 10, 1998)

Abstract: Significant coseismic and postseismic deformation lasting about 10 days was observed by strainmeters and GPS measurements at sites more than 150km apart from the 1994 far off Sanriku earthquake (MJMA 7.5) on December 28, 1994. Modeling the crustal deformation by simple rectangular faults in a half space, seismic moments of the main shock and the largest aftershock (MJMA 7.1) were estimated as 5.9×10^{20}N•m and 9.2×10^{19} N•m, respectively. The cumulative amplitudes of the postseismic deformations until the occurrence of the largest aftershock (MJMA 7.1) on Jan. 7, 1995 are 30% of the coseismic ones on average. The polarities of postseismic deformations are mostly the same as those of the coseismic ones. Therefore, the postseismic deformations can be interpreted by aseismic sliding on a fault similar to that of the main shock.

1. Introduction

The 1994 far off Sanriku earthquake (MJMA 7.5) occurred off the coast of Sanriku on December 28, 1994. Its focal mechanism and aftershock distribution are shown in Figure 1 and suggest that the earthquake is a low-angle thrust-fault on the plate boundary and one of the typical interplate earthquakes in the subduction zone of the Pacific plate.

Miura *et al.* (1995) reported that strain steps associated with this earthquake and its largest aftershock (MJMA 7.1) were observed by extensometers installed in vaults and borehole strainmeters in the Tohoku district, and that the coseismic displacements observed by GPS could be explained by simple rectangular fault models for these earthquakes. They further pointed out that postseismic deformations were observed both by GPS and by the extensometeres. Tsuji *et al.* (1995) also found that GPS stations of the Geographical Survey Institute, Japan (GSI) near the aftershock area were displaced eastward at the time of the main shock and that they continued their eastward displacement with an exponential decay as a function of time.

[1] Research Center for Prediction of Earthquakes and Volcanic Eruptions, Faculty of Science, Tohoku University, Sendai 980-8578
[2] Geographycal Survey Institute, Tsukuba, Ibaraki 305-0811
* Present address: Tohoku Regional Survey Department, Geographycal Survey Institute, Sendai 983-0842

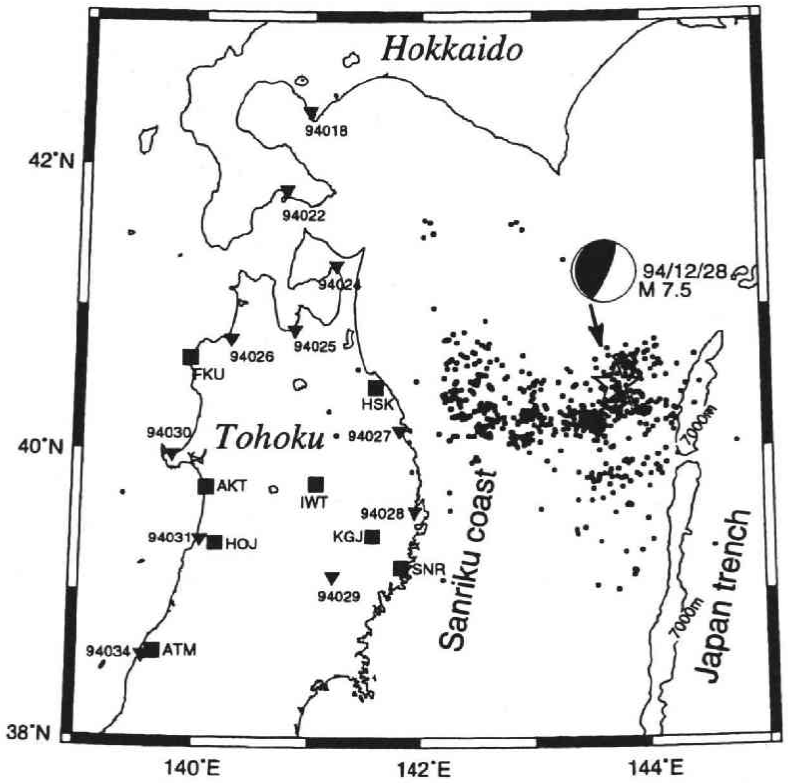

Fig. 1. Hypocenter distribution of the 1994 far off Sanriku earthquake and its aftershocks determined by the network of Tohoku University with the location of GPS sites. The focal mechanism inserted shows the best double-couple solution obtained by Dziewonski *et al.* (1995). Inverse triangles and squares are GPS stations operated by GSI and Tohoku University, respectively.

In this paper, first, we describe the procedure for noise reduction of the strain data obtained with extensometers and borehole strainmeters. Next, we estimate model parameters of simple rectangular faults for the main shock and the largest aftershock by a grid-search inversion method using data obtained by strain and GPS measurements. Finally, we discuss the temporal change in short-term postseismic deformations observed before the largest aftershock by assuming postseismic sliding on the model fault estimated for the main shock.

2. Data

2.1 Observation Network

Tohoku University staff carry out strain and tilt measurements at more than 25 stations. The instruments are extensometers and water-tube tiltmeters in observational vaults or borehole-type strain- and tilt-meters. It is unfortunate that both water-tube tiltmeters and borehole-type tiltmeters frequently show unaccountable

behavior when they experience strong ground motions due to earthquakes. In addition, some stations were not in operation when the main shock took place. In the present study, we therefore use only the data observed by extensometers and borehole strainmeters with few recording gaps. Figure 2 shows the location map of the stations used in this study. The pertinent information about the stations is given in Tables 1 and 2 (cf. Faculty of Science, Tohoku University, 1995)

In 1994 a regional GPS network consisting of eleven stations was operated in northeastern Japan by Tohoku University (Miura *et al.*, 1994). GSI established a nationwide GPS array of 100 stations named GRAPES (GPS Regional Array for PrEcise Surveying/Physical Earth Science) (Miyazaki *et al.*, 1996). GPS data from both networks are used in this study and the locations of GPS stations are shown in Figure 1. GPS receivers of both networks are TOPCON GP-R1DY (equivalent of Ashtech Z-12) capable of decoding P and Y codes. GPS data of each network are routinely analyzed to obtain daily baseline vectors at each institution separately with the same GAMIT

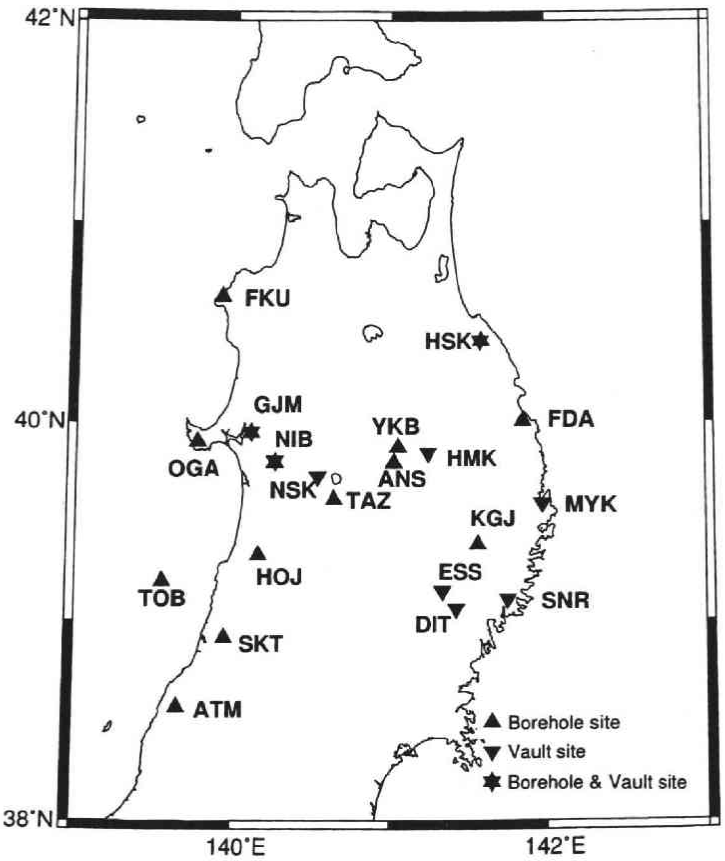

Fig. 2. Location map of stations for continuous observations of crustal deformations used in this study. ESS is operated by National Astronomical Observatory. The others are operated by Tohoku University.

Table 1. Location of the stations and the pertinent data of extensometers in vault.

Station code	Station name	Latitude (°N)	Longitude (°E)	Altitude (m)	Start date*	EXT. 1		EXT. 2		EXT. 3		EXT. 4	
						Auimuth**	Longth (m)	Azimuth	Length (m)	Azimuth	Length (m)	Azimuth	Length (m)
OGA	Oga	39.898	139.779	260	May, 1967	140.4	26.65	50.6	23.65	5.6	29.1		
NIB	Nibetsu	39.803	140.268	243	Dec., 1968	23.3	25.1	111.2	24.1	67.8	27.4		
HMK	Himekami	39.848	141.243	640	Oct., 1971	51.4	30	141.2	30	10.6	30		
MYK	Miyako	39.590	141.982	120	Aug., 1969	78.4	25	157.5	25	78.5	25	168.6	25
SNR	Sanriku	39.107	141.758	519	Sep., 1969	25	25	81	25	171	25	81	25
GJM	Gojome	39.952	140.116	105	Sep., 1982	30.8	14.7	120.8	13.4	165.7	17.69		
NSK	Nishiki	39.728	140.546	260	Sep., 1982	146.0	14.72	56.0	13.38	10.9	17.68		
TAZ	Tazawako	39.612	140.654	170	Sep., 1982	165.7	14.69	75.8	13.38	30.7	17.69		
SWU	Sawauti	39.486	149.793	445	Sep., 1982	132.4	14.69	42.4	13.4	177.5	17.69		
HAN	Hanamaki	39.373	140.943	260	Mar., 1995	18.3	15	153.3	15	63.3	15		
KRS	Kurosawajiri	39.262	141.153	150	Jan., 1983	88.7	14.7	178.7	13.39	133.7	17.7		
DIT	Daito	39.061	141.426	400	Jan., 1982	86.5	14.71	176.6	13.41	131.5	16.95		
KSN	Kesennuma	39.974	141.534	280	Jan., 1982	81.8	14.68	171.6	13.37	36.8	17.01		
HSK	Hashikami	40.412	141.584	355	Jun., 1977	87	3	177	3	132	4		
ESS***	Esashi	39.148	141.335	393	Jun., 1979	0	35.77	90	35.69	45	50.67		

ESS is established by Mizusawa Astrogeodynamics Observatory, National Astronomical Observatory.

* The date at which observation was started.

** Measured clockwise from the north together in degree.

*** This station code is used only in this study for the sake of convenience.

Table 2. Location of the stations with borehole strainmeters.

Station code	Station name	Latitude (°N)	Longitude (°E)	Elevation (m)*	Start date**	Approx. depth (m)
TAZ	Tazawako	39.612	140.655	70	Oct., 1982	100
OGA	Oga	39.900	139.767	170	Dec., 1985	200
NIB	Nibetsu	39.800	140.267	40	Dec., 1985	200
HOJ	Honjo	39.333	140.167	−115	Dec., 1985	200
ANS	Ainosawa	39.797	141.027	150	Nov., 1994	300
YKB	Yakebashiri	39.874	141.053	250	Nov., 1994	300
FKU	Fukaura	40.632	139.915	−320	Dec., 1994	500
TBS	Tobishima	39.195	139.557	−440	Oct., 1994	500
SKT	Sakata	38.917	139.950	−370	Oct., 1994	500
ATM	Atsumi	38.569	139.662	−360	Oct., 1994	500
FDA	Fudai	40.009	141.858	−245	Dec., 1994	500
KGJ	Kitakami	39.386	141.565	−120	Dec., 1994	500

* Elevation of the sensors.
** The date at which observation was started.

software (King and Bock, 1995).

2.2 Noise Reduction of Strain Data

The data obtained by continuous measurements of strains and tilts are contaminated generally by noise due to meteorological phenomena, say, rainfall and changes in atmospheric pressure and temperature. This noise should be removed from the observed data before tectonic analysis. Generally speaking, it is almost impossible, however, to estimate the noise from all sources. The effects of earth tides and atmospheric pressures have been investigated well and can be removed from the observed data.

We use BAYTAP-G (Tamura *et al.*, 1991) to estimate the effects of earth tides and atmospheric pressures. The program evaluates the amplitude factor and phase of each constituent of earth tides and the response coefficients to the associated data of atmospheric pressure. Figure 3 shows an example of the result of BAYTAP-G applied to the 1-hour sampling data of the 1st extensometer at HMK to decompose the original data into tidal, response, trend, and irregular components.

The scheme for the reduction of tidal and pressure effects from strain data is summarized as follows: First, the amplitude factor and phase of each tidal constituent and the response coefficient to atmospheric pressure changes are determined by using the observed data in a period of presumably low noise-level without any artificial noise, during which there seem to exist no significant effects of precipitation. Next, the time series of the theoretical tides for the whole period under investigation are theoretically synthesized by the use of the program TIDE4N (Tamura, personal communication), in which the amplitude factors and phases of tidal constituents determined previously are used as input data. Further, the responses to the atmospheric pressure changes are

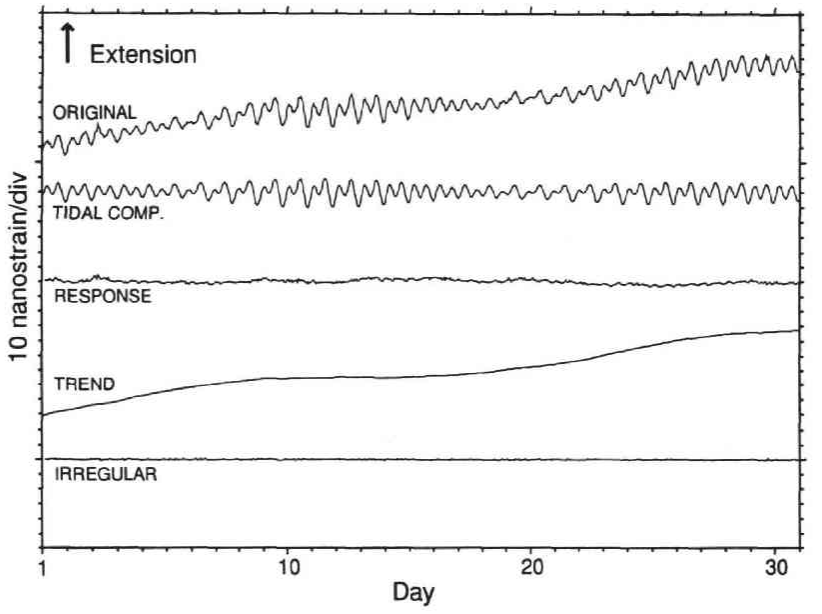

Fig. 3. An example of decomposition by BAYTAP-G. The components are from the top: original data, tide, response to pressure, trend, and irregular noise. The original data is observed with the 1st extensomter at HMK from July 1, 1994, to July 30, 1994.

calculated using the response coefficient determined previously by BAYTAP-G. Subtracting these two components from the original observed time series, we finally get the data free from earth tides and the effect of atmospheric pressures.

Figure 4 exhibits the final results of strain changes by extensometers and strainmeters obtained through the procedure explained above for the period from December 19, 1994 to January 31, 1995. It is found that this processing of noise reduction considerably improves the signal to noise ratio. It is further noted that in addition to coseismic strain steps for the main shock on December 28, 1994 and for the largest aftershock occurring on January 7, 1995, significant postseismic strains decaying exponentially are clearly seen on the strain records of HSK, HMK, ESS, DIT, and FDA in Figure 4, where the postseismic strain changes observed at the other stations are not considered significant because of their apparently poor signal to noise ratio. The sense of postseismic strain changes is mostly the same as that of coseismic strain steps for the main shock at respective components.

3. Coseismic Faulting Models

In this section we will construct simple models of coseismic faulting for the largest aftershock as well as for the main shock so as to satisfy the observed data of GPS and

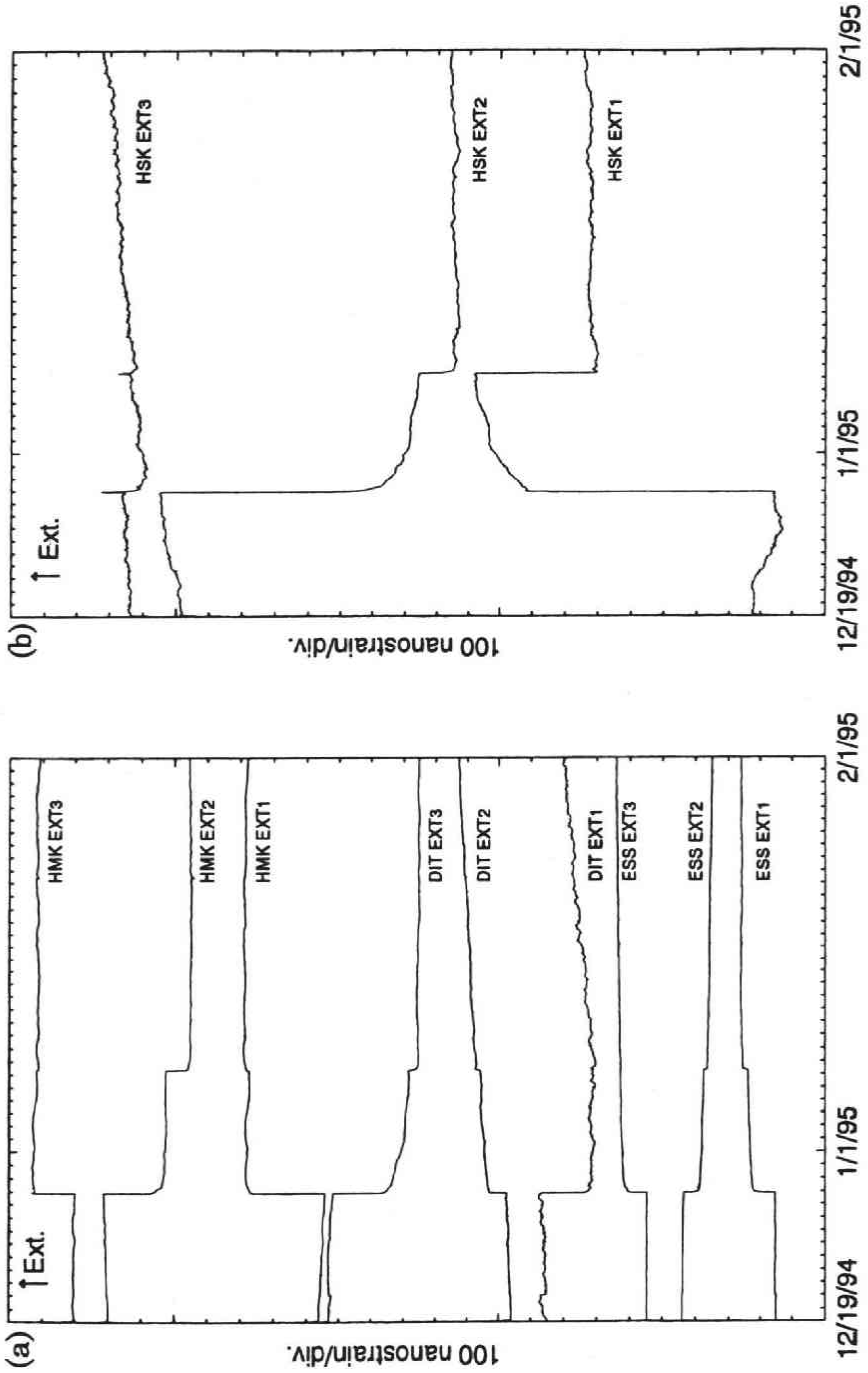

Fig. 4. Strain data corrected for earth tides and the effect of atmospheric pressure. EXTn means the n-th component of an extensometer. BSMD means a borehole strainmeter.

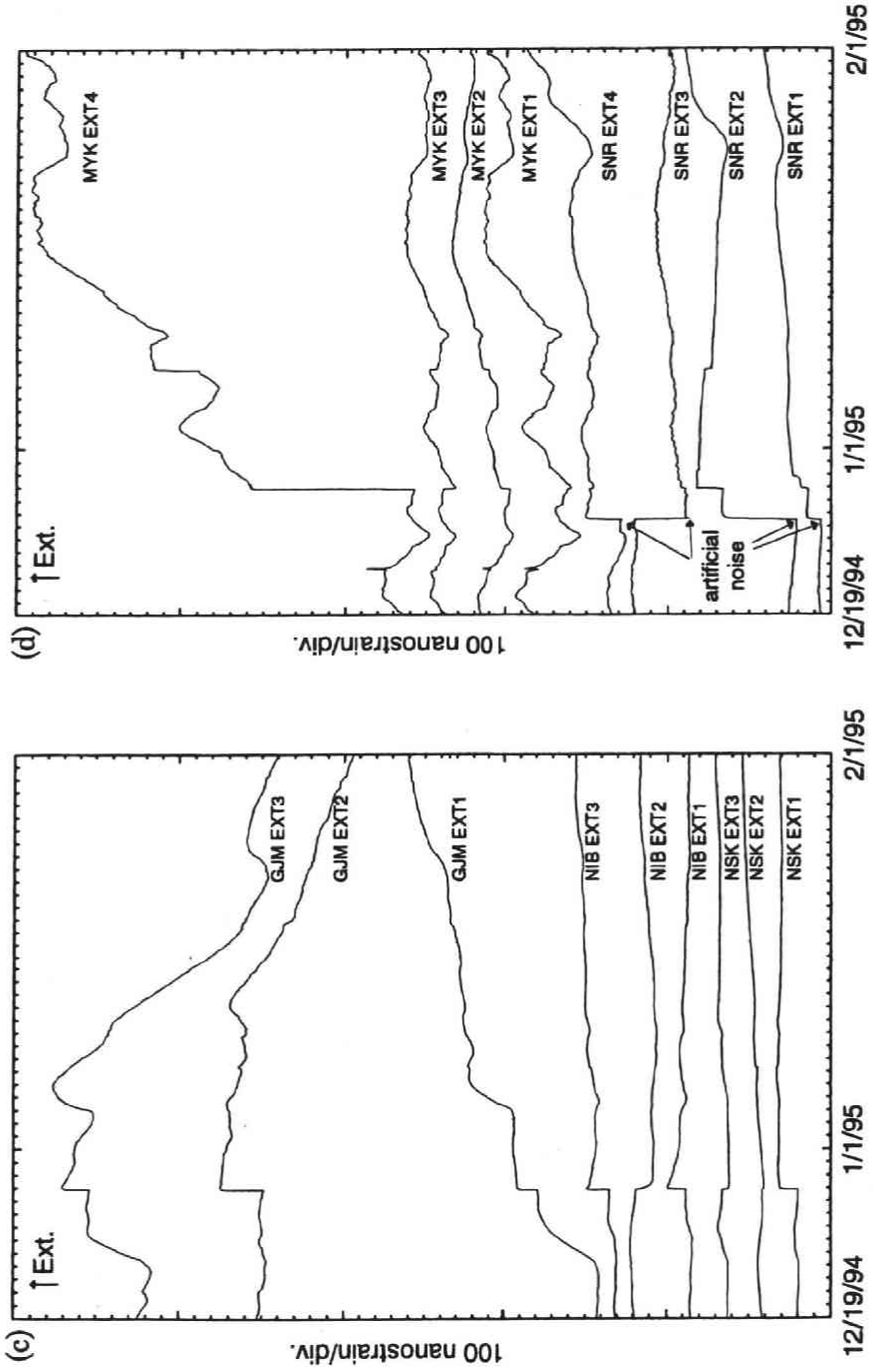

Fig. 4. (Continued)

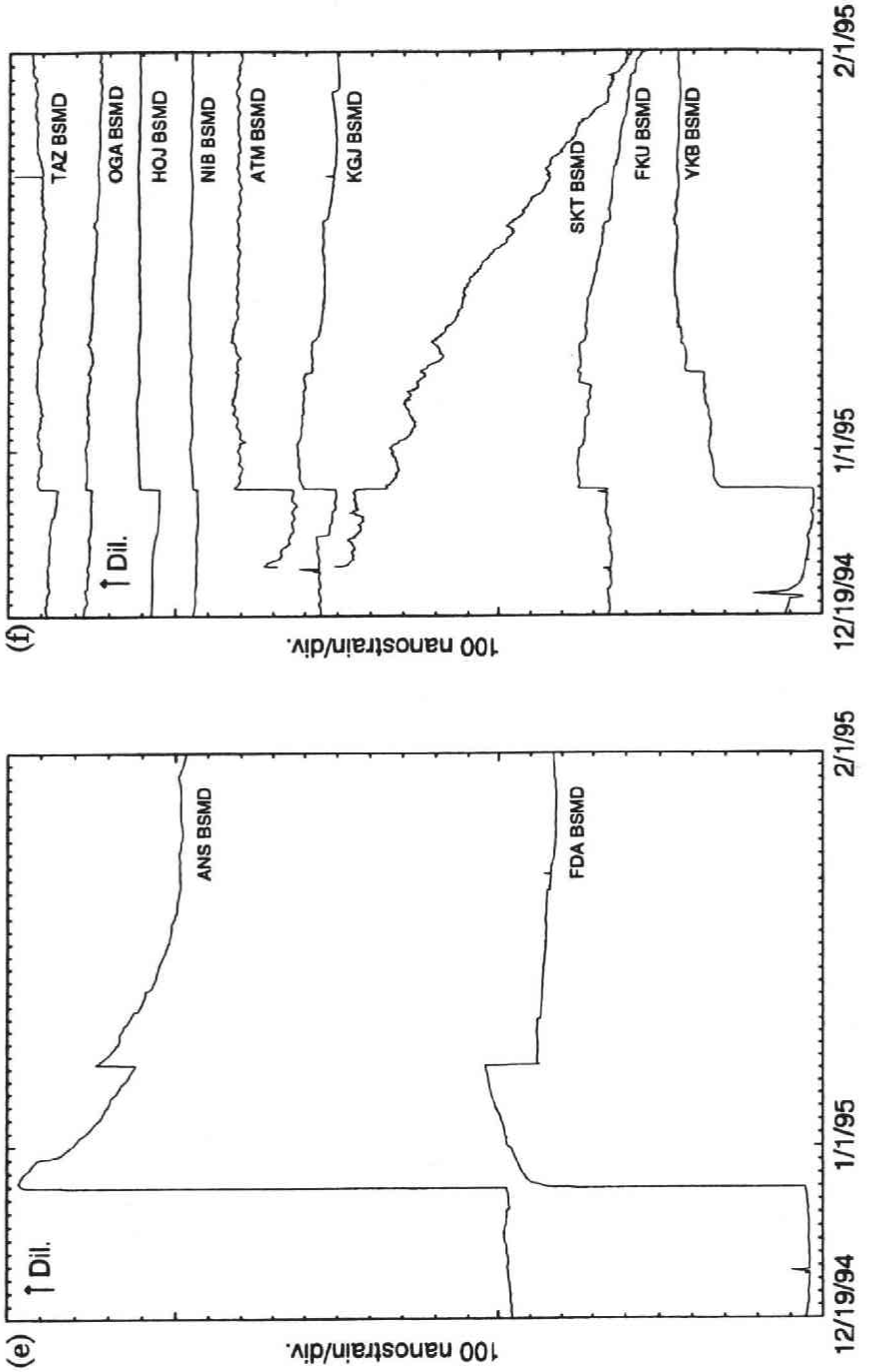

Fig. 4. (Continued)

strain changes. For estimation of the unknown model parameters of coseismic faults rectangular in shape, a grid search technique is used to minimize the sum of squares of residuals both for NS- and EW-components of baseline vectors observed by GPS and for the amplitudes of strain changes observed by extensometers and strainmeters. The changes in each baseline length are divided by the length between the two endpoints in order to make the dimension of GPS data consistent with strain data. From the recent experiences, the GPS data are generally considered to be more reliable than the data of strain changes. In applying a least squares technique, therefore, we assign the GPS data a weight two times as large as that of the strain data.

The amplitudes of coseismic strain steps are read by eye from 1-hour sampling records only for stations with high signal to noise ratios. In the case of GPS data the coseismic change is defined by the difference between the daily solution of the preceding day and that of the next day. That is to say, it is the difference between the daily solution of December 27 and that of December 29 in the case of the main shock. The station ATM is selected as a reference site for the network of Tohoku University, and the station 94034 is for the network of GSI. We used Okada's(1985) formulation to calculate surface strains and displacements due to a finite rectangular fault in a half-space.

Considering that the main shock and the largest aftershock can be regarded as typical plate-boundary earthquakes from their locations and focal mechanisms, we assume that their fault planes are on the boundary between the subducting Pacific plate and the continental (supposedly, the North American) plate. Therefore, the dip directions and the dip angles of fault planes are fixed both for the main shock and for the largest aftershock.

It is known that the plate boundary is bending significantly at around 143°E in longitude in the region under consideration (Umino *et al.*, 1995a, b). Since the distribution of aftershocks spreads from about 144°E to the vicinity of 142°E, a two-segment fault should be assumed for the main shock as shown in Figure 5, where the dip angle of the fault plane is 10 degrees for the eastern segment and 35 degrees for the western one according to the result by Miura *et al.* (1995). To decrease the number of unknown parameters to be estimated, we fix the locations and the sizes of these two fault segments in the case of the main shock by taking account of the aftershock distribution (cf. Figure 5 and Table 3). Thus, the number of unknown parameters for the main shock is four; the strike and dip components of slip vectors on the two individual fault segments. The step in the amount of slip for the grid search is taken to be 0.02 m.

In the case of the largest aftershock, on the other hand, a fault model of a single segment seems to be sufficient considering its magnitude and aftershock distribution. Because of the simplest fault configuration, the location, say, the latitude and the longitude of the center point of the upper side, and the size, say, length and width, of the rectangular fault are also taken as unknown parameters in addition to the strike and dip components of the slip vector. Therefore, the number of unknown parameters to be estimated is six in the case of the largest aftershock. The steps in the amount of slip,

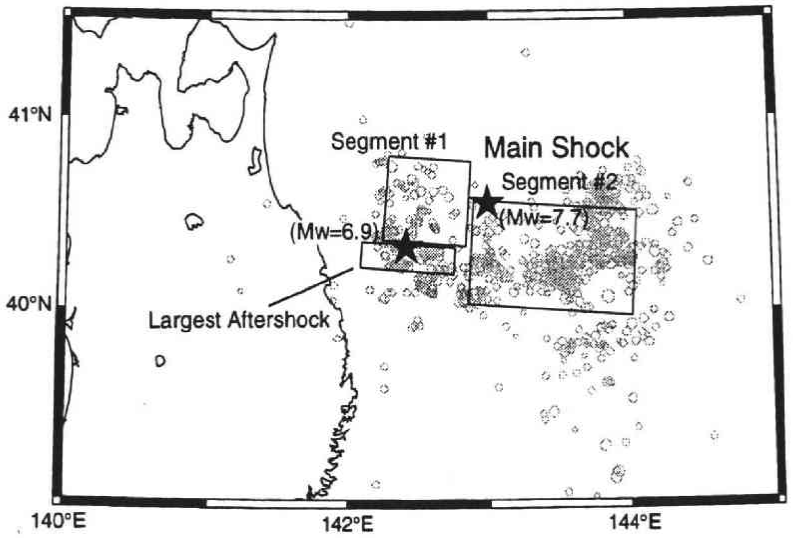

Fig. 5. Fault geometry of model faults in grid search analyses. Stars are the centroids of the 1994 far off Sanriku earthquake and the largest aftershock (Dziewonski *et al.*, 1995, 1996). Open circles are epicenters determined by Tohoku University for the period from December, 28, 1994 to February 1, 1996.

Table 3. The optimum fault parameters of the 1994 far off Sanriku earthquake and its largest aftershock obtained from strain and GPS data.

	Main Shock		Largest Aftershock
	Segment #1	Segment #2	
Mo	4.3×10^{20} Nm	1.6×10^{20} Nm	9.2×10^{19} Nm
Mw	7.8		7.2
Strike	N184° E	N184° E	N184° E
Dip Angle	8	35	35
Rake Angle	76°*	84°*	99°*
Length × Width	60 km × 100 km	50 km × 60 km	15 km* × 80 km*
Dislocation	1.81 m*	1.35 m*	1.92 m*
Latitude	40.24°N	40.55°N	40.25°N*
Longitude	144.04°E	142.85°E	142.75°E*
Depth	10 km	24 km	31 km

Asterisks indicate independent unknown parameters in the least squares analysis.
Rigidity is assumed to be 4.0×10^{10} Nm^{-2}. The locations of the faults are given at midpoint of upper edges of faults.

the length, the width, and the location for the grid search are taken to be 0.02 m, 5 km, 5 km, and 0.05°, respectively.

The results of the least squares solutions for these events are tabulated in Table 3.

The seismic moment of the main shock (5.9×10^{20}N·m) is slightly larger than that of Harvard CMT solution (4.9×10^{20}N·m, Dziewonski *et al.*, 1995). The slip direction obtained indicates thrust faulting with a slight left-lateral strike-slip component, similarly to the above mentioned CMT solution. In the case of the largest aftershock the seismic moment estimated in this study (9.2×10^{19}N·m) is three times as large as that of the Harvard CMT solution (3.3×10^{19}N·m, Dziewonski *et al.*, 1996). Another feature of our solution to be mentioned is the very small aspect ratio of the rectangular fault, as shown in Figure 5. The estimated width of the fault in the east-west direction seems to be a little too long in comparison with the aftershock distribution of the largest aftershock. However, the estimated slip direction dominated by a thrust component is reasonable for an earthquake occurring on a subducting plate boundary, and the estimated fault area contains the centroid of the earthquake given by the Harvard CMT solution, as seen in Figure 5.

4. Interpretation of Observed Postseismic Deformations

Miura *et al.* (1995) have shown from their analysis of GPS data that the temporal variation of the baseline vector between ATM and HSK for about 40 days after the main shock is well explained by a model in which a slip with an exponentially decaying time function is assumed on the same fault as that of the main shock. They found further that their model explains also strain changes observed by extensometers and borehole strain meters to some extent.

Figures 6 and 7 demonstrate clear postseismic deformation on the observed time series of strains and relative displacements by GPS. It may be understood from the figures that except for a few cases the senses of postseismic deformations are the same as those of coseismic steps of the main shock on the respective components, and that the amplitude ratios of the postseismic deformation accumulated until the occurrence of the largest aftershock to the coseismic steps of the main shock are about 30% on average. This suggests the validity of the simple interpretation by Miura *et al.* (1995) that the observed postseismic deformation was caused by an after-slip on the same fault as that of the main shock.

Following the procedure used by Miura *et al.* (1995), we synthesize the theoretical time series to compare them with the observed ones. The assumption made for the theoretical simulation is that the postseismic sliding takes place in the same way as the coseismic slip of the main shock except for its time dependence. More precisely speaking, the two-segment fault model estimated for the main shock in the preceding section is used for the postseismic sliding. The locations, the sizes, and the slip directions of the two fault segments are thus given by the results of the preceding section. The time dependence of the postseismic sliding is assumed by;

$$\boldsymbol{u}(t)=C\boldsymbol{u}_1\left\{1-\exp\left(-\frac{t-\tau_1}{T}\right)\right\}\mathrm{H}(t-\tau_1) \tag{1}$$

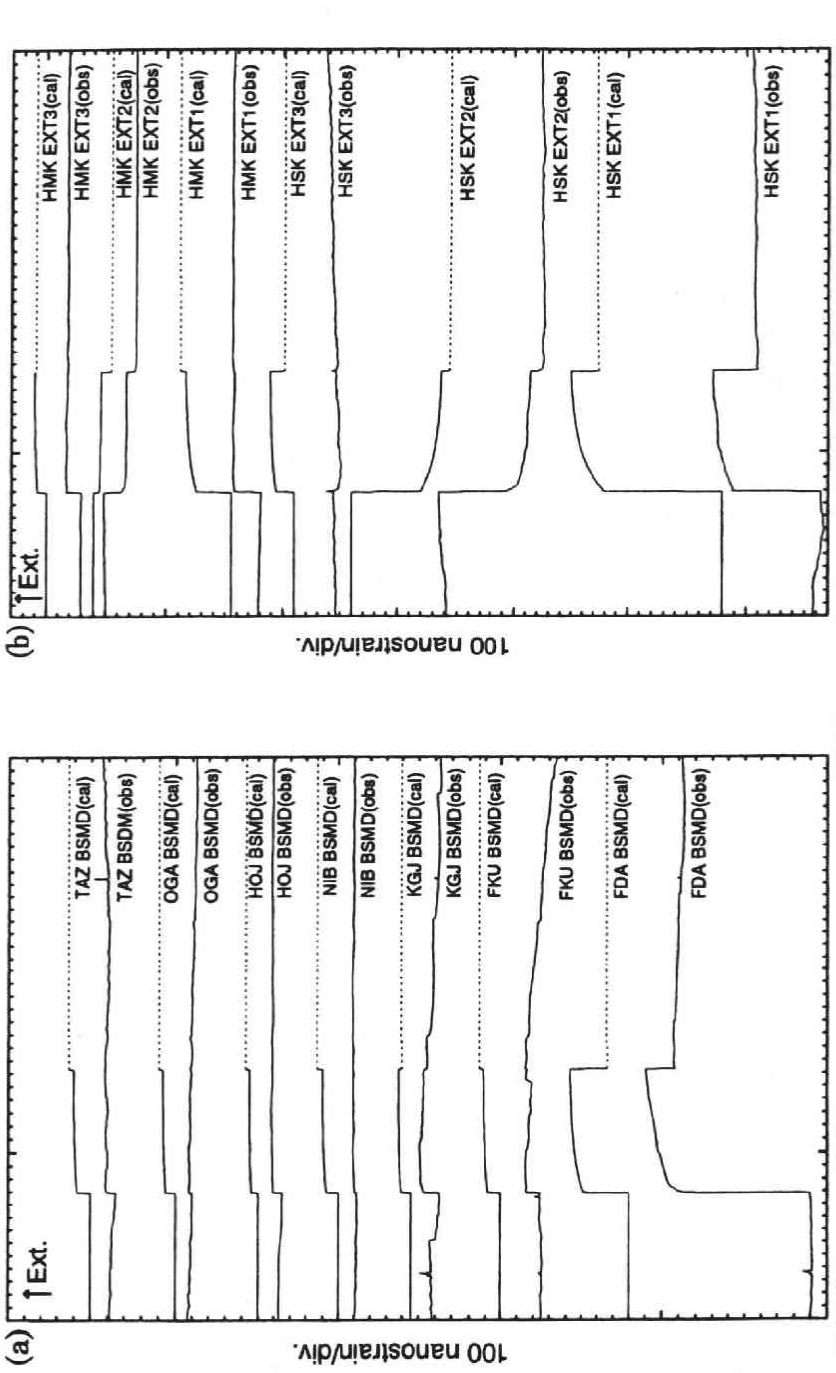

Fig. 6. The observed time series (obs) of strains in comparison with the theoretical ones (cal) calculated for the coseismic and postseismic fault model estimated. (a) TAZ, OGA, HOJ, NIB, KGJ, FKU, and FDA. (b) HSK and HMK. (c) DIT and ESS.

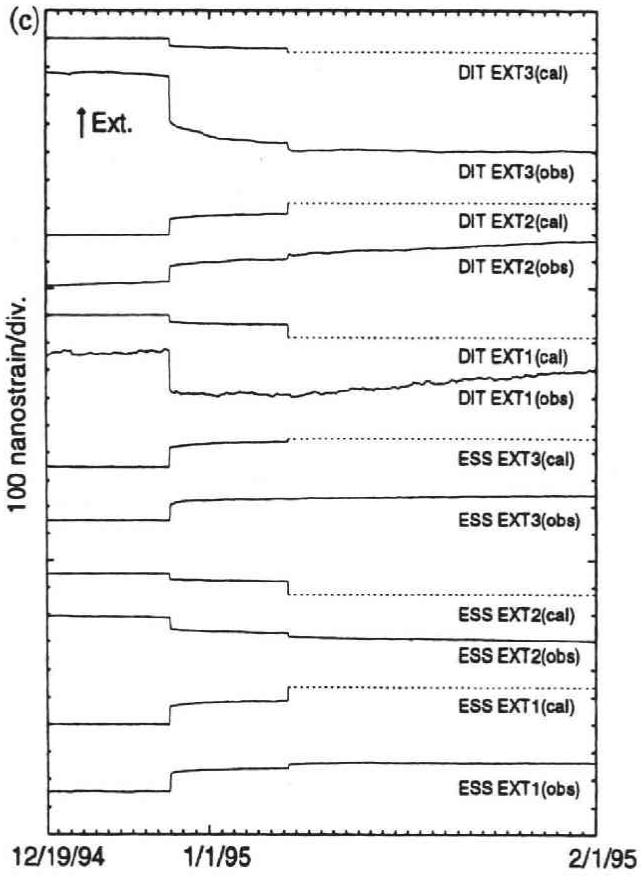

Fig. 6. (Continued)

where $\boldsymbol{u}(t)$ is the slip vector as a function of time t for postseismic sliding, $\boldsymbol{u}_1$ is the slip vector estimated for the main shock, C is a constant to determine the ratio of postseismic slip to coseismic one, τ_1 is the origin time of the main shock, T is a time constant, and $\mathrm{H}(t)$ is a unit step function.

Since the spatial pattern of postseismic faulting is assumed to be the same as that of the coseismic faulting for the main shock, the constant C should be given by the average amplitude ratio of 30% found previously for the postseismic deformations and the coseismic steps. Thus $C=0.3$ is adopted. The time constant is determined on the basis of trial and error, and $T=3$ days is found to be appropriate.

The theoretical time series thus synthesized are shown and compared with the observed ones in Figures 6 and 7, where the steps in the theoretical time series are evaluated from the fault models estimated previously for the main shock and for the largest aftershock. It turns out from the figures that the observed time series by strain and GPS measurements are qualitatively well explained by the theoretical calculation in spite of the simplicity of the present model. Although our model of postseismic sliding

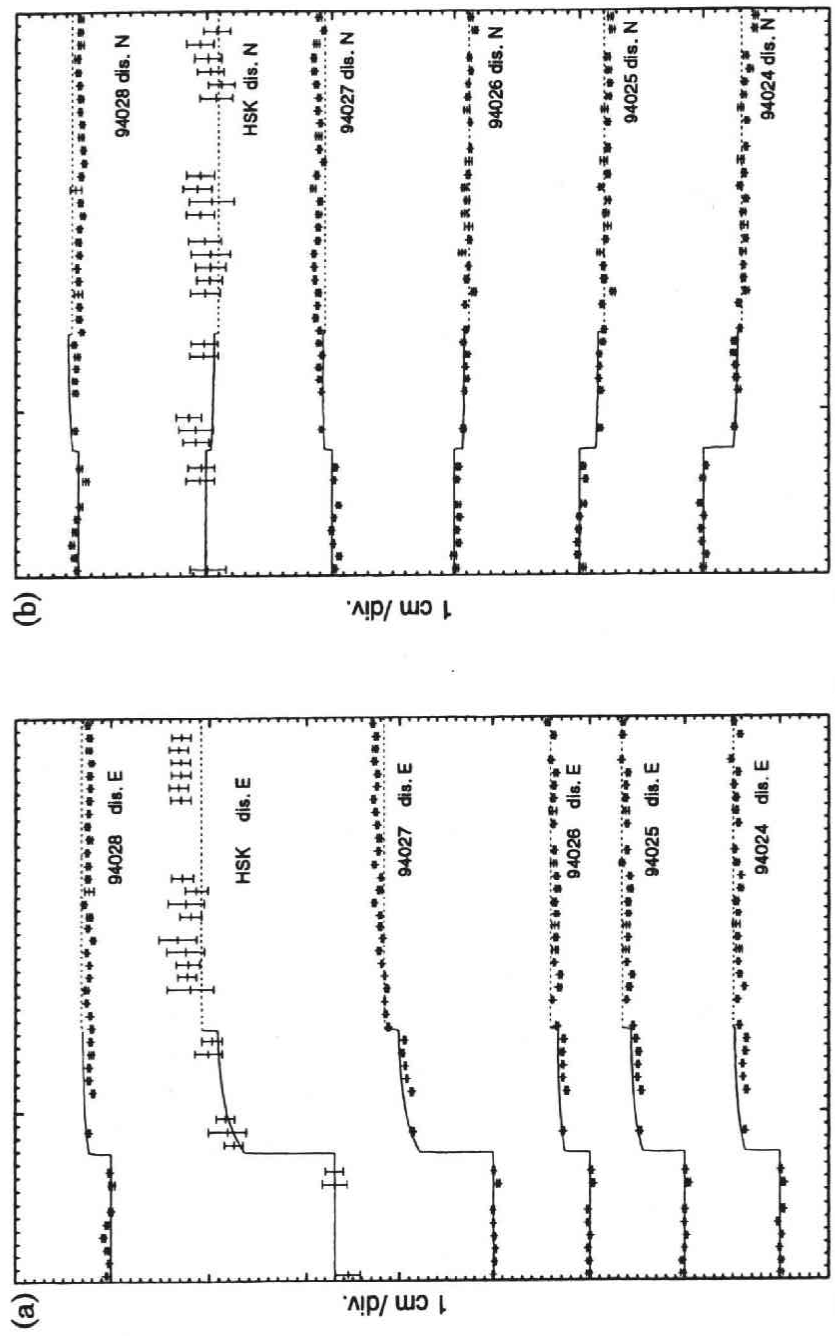

Fig. 7. The observed time series (short dash with error bar) of relative displacement by GPS in comparison with the theoretical ones (solid and dotted line) where 94028 (Miyako), 94027 (Kuji), 94026 (Ajigasawa), and 94024 (Mutsu) are relative to 94034 (Atsumi) and HSK (Hashikami) relative to ATM (Atsumi). (a) and (b) stand for NS and EW components, respectively. Error bars indicates one standard deviation.

was obtained from the data for the period between the main shock and the largest afterschock, the synthesized time series are extrapolated and shown in Figures 6 and 7 up to the end of January, 1995, for the sake of reference.

5. Discussion and Conclusion

Figure 8 shows all the observed strain steps in comparison with the theoretical ones expected for the estimated model in the case of the main shock. Although many of the observed steps are well explained by the model, some observations are different from the theories even in polarity. Okada (1980) has pointed out that the amplitudes of cosesmic strain steps measured with extensometers and strainmeters often disagree with those theoretically calculated for a fault model, and that their polarities are occasionally reversed. An example of rather poor reliability in strain-step measurements is found in Figure 4(d); the coseismic steps due to the main shock are significantly different between EXT2 and EXT4 at SNR station although they are installed only tens of meters apart with almost the same azimuth. We have therefore excluded from the grid search

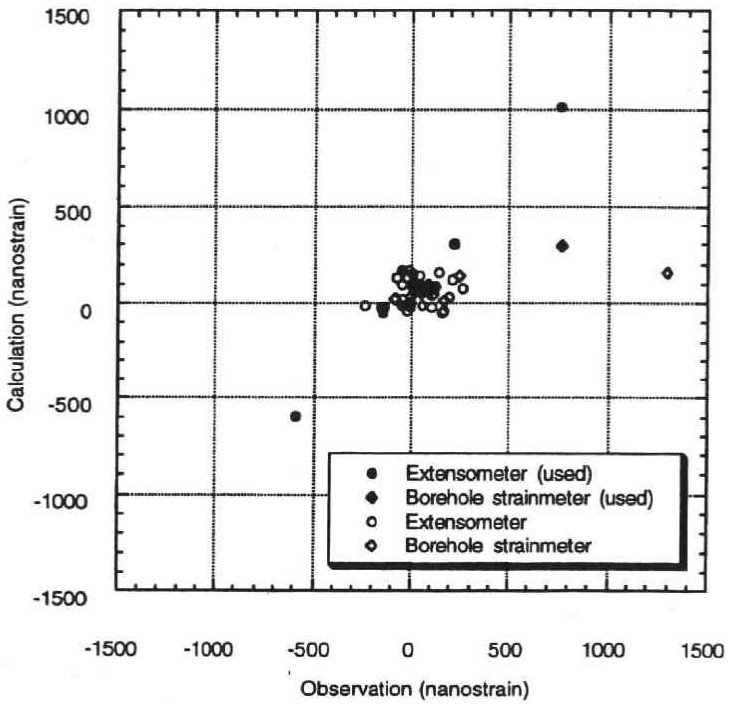

Fig. 8. Comparison of the observed coseismic step amplitudes with the theoretical ones calculated from the estimated fault model for the 1994 far off Sanriku earthquake (MJMA7.5). Solid symbols are the data to determine the fault model, and open symbols are the data obtained at unstable stations and not used for the model construction.

analysis obviously unreliable data of strain steps, which are indicated by open symbols in Figure 8. General agreement in steps between the observation and the theory is seen in Figures 6 and 7. The agreement is quite satisfactory particularly for the GPS data in the case of the main shock.

The seismic moment estimated for the largest aftershock does not seem reasonable, as stated before. Considering that we obtained a very satisfactory result of seismic moment in the case of the main shock, the main reason for the disagreement may be poor signal to noise ratios of the observed data in the case of the largest aftershock. This may easily be understood from Figures 6 and 7, where many of the observed steps for the largest aftershock are marginal to the noise levels particularly in the case of GPS data. However, the location, the size and the slip direction of the estimated fault model are reasonable. We consider that the obtained result is more satisfactory than expected previously, because it is generally considered that the data of crustal deformations observed at distances large compared with the source size have poor resolution and are explained satisfactorily well by a point source model. It is, therefore, concluded that the data of crustal deformations are useful for the analyses of the coseismic faulting process from the present study.

The observed postseismic crustal deformations between the main shock and the largest aftershock are found to be explained qualitatively by a simple model of postseismic sliding on the same two-segment fault as that estimated for the main shock. It is thus concluded that until the occurrence of the largest aftershock the fault of the main shock continued to slide aseismically and did not significantly expand its area to a first approximation. It may be naturally expected, however, that the faulting area should have enlarged as time went on. An evidence for this is significant enlargement of aftershock area by the occurrence of the largest aftershock.

Long-term postseismic deformations lasting for more than one year after the occurrence of the main shock were observed by GPS measurements (cf. Tsuji *et al.*, 1995 ; Heki *et al.*, 1997). Significant strain changes lasting for such a long period of one year were not detected, however, either with borehole strainmeters or with extensometers. Nishimura (1997) has discussed the characteristics of postseismic deformations observed for one-year period after the main shock. According to his result the strain changes expected theoretically for his postseismic sliding model are about 300 nanostrains at the largest. This amount of strain changes for one-year period does not seem to be detectable with strainmeters and extensometers because of large trends and/or large annual variations usually found for strain observations.

Acknowledgment : Authors are grateful to Professors H. Hamaguchi, A. Hasegawa, and M. Ohtake for their valuable discussion. They are also indebted Professor M. Wyss for his critically reviewing the manuscript and making valuable comments. They thank all staffs and students of Research Center for Prediction of Earthquakes and Volcanic Eruptions, Faculty of Science, Tohoku University for their helpful comments.

References

Dziewonski, A., G. Ekström and M. Salganik, 1995 : Centroid-moment tensor solutions for October-December 1994, *Phys. Earth Planet. Inter.*, **91**, 187-201.

Dziewonski, A., G. Ekström and M. Salganik, 1996 : Centroid-moment tensor solutions for January-March 1995, *Phys. Earth Planet. Inter.*, **93**, 147-157.

Faculty of Science, Tohoku University, 1995 : Crustal movement, *Technical Report of Earthquakes and Volcanoes*, **25**, 74-102.

Heki, K., S. Miyazaki and H. Tsuji, 1997 : Silent fault slip following an interplate thrust earthquake at the Japan Trench, *Nature*, **386**, 595-598.

King, R.W. and Y. Bock, 1995 : *Documentation for the GAMIT GPS analysis software, Release 9.40-November 1995*, Mass. Inst. of Technol. and Univ. Calif. San Diago.

Miura, S., K. Tachibana, K. Hashimoto, T. Sato, S. Hori, E. Murakami, T. Kono, K. Nida and T. Hirasawa, 1994 : Continuous GPS observation in Tohoku district : The outline of the new observation system and the preliminary results (in Japanese), *Abstract of Seism. Soc. Japan*, No. 2, 173.

Miura, S., K. Tachibana, K. Hashimoto, T. Sato, S. Hori, E. Murakami, T. Kono, K. Nida, T. Nishimura and T. Hirasawa, 1995 : Faulting process of the 1994 Far East Off Sanriku earthquake inferred from GPS observation (in Japanese with English abstract), in *Investigation on the 1994 Sanriku-harukaoki Earthquake and the Earthquake Disaster Caused by it* (*ed.* A. Hasegawa), published by support of Grant-in-Aid for Scientific Research, Project No. 06306019, 97-104.

Miyazaki, S., H. Tsuji, Y. Hatanaka, Y. Abe, A. Yoshimura, K. Kamada, K. Kobayashi, H. Morishita and Y. Iimura, 1996 : Establishment of the nationwide GPS array (GRAPES) and its initial results on the crustal deformation of Japan, *Bull. Geog. Surv. Inst.*, **42**, 27-41.

Nishimura, T., 1996 : The spatiotemporal distribution of coseismic and postseismic slip associated with the 1994 Far Off Sanriku Earthquake, Master Thesis, Tohoku Univ., Sendai, pp.127.

Okada, Y., 1980 : Strain- and tilt-steps associated with the Izu-Hanto-Oki earthquake of 1974 and Izu-Oshima-Kinkai earthquake of 1978 (in Japanese with English abstract), *J. Seism. Soc. Japan.*, **33**, 529-539.

Okada, Y., 1985 : Surface deformation due to shear and tensile faults in a half-space, *Bull. Seism. Soc. Am.*, **75**, 1135-1154.

Tamura, Y., T. Sato, M. Ooe and M. Ishiguro, 1991 : A procedure for tidal analysis with a Bayesian information criterion, *Geophys. J. Int.*, **104**, 507-516.

Tsuji, H., Y. Hatanaka, S. Miyazaki and F. Webb, 1995 : Postseismic deformations after 1994 Sanriku Haruka-oki earthquakes monitored by GSI's nationwide GPS array (in Japanese), *Abstract of Geod. Soc. Japan*, 149-150.

Umino, N., A. Hasegawa and T. Matsuzawa, 1995a : sP depth phase at small epicentral distances and estimated subducting plate boundary, *Geophys. J. Int.*, **120**, 356-366.

Umino, N., A. Hasegawa and T. Matsuzawa, 1995b : Aftershock focal depths of the 1994 Far Off Sanriku earthquake estimated from sP depth phase (in Japanese with English abstract), in *Investigation on the 1994 Sanriku-harukaoki Earthquake and the Earthquake Disaster Caused by it* (*ed.* A. Hasegawa), published by support of Grant-in-Aid for Scientific Research, Project No. 06306019, 23-37.